Mice with a Deletion of Rsph1 Exhibit a Low Level of Mucociliary Clearance and Develop a Primary Ciliary Dyskinesia Phenotype

Yin, Weining; Livraghi-Butrico, Alessandra; Sears, Patrick R; Rogers, Troy D; Burns, Kimberlie A; Grubb, Barbara R; Ostrowski, Lawrence E . American Journal of Respiratory Cell and Molecular Biology (Online) ; New York Vol. 61, Iss. 3, (Sep 2019): 312–321.

ABSTRACT (ENGLISH)

Primary ciliary dyskinesia (PCD) is a genetically and phenotypically heterogeneous disease caused by mutations in over 40 different genes. Individuals with PCD caused by mutations in RSPH1 (radial spoke head 1 homolog) have been reported to have a milder phenotype than other individuals with PCD, as evidenced by a lower incidence of neonatal respiratory distress, higher nasal nitric oxide concentrations, and better lung function. To better understand genotype–phenotype relationships in PCD, we have characterized a mutant mouse model with a deletion of Rsph1. Approximately 50% of cilia from Rsph1$^{/}$ cells appeared normal by transmission EM, whereas the remaining cilia revealed a range of defects, primarily transpositions or a missing central pair. Ciliary beat frequency in Rsph1$^{/}$ cells was significantly lower than in control cells (20.2 ± 0.8 vs. 25.0 ± 0.9 Hz), and the cilia exhibited an aberrant rotational waveform. Young Rsph1$^{/}$ animals demonstrated a low rate of mucociliary clearance in the nasopharynx that was reduced to zero by about 1 month of age. Rsph1$^{/}$ animals accumulated mucus in the nasal cavity but had a lower bacterial burden than animals with a deletion of dynein axonemal intermediate chain 1 (Dnaic1$^{/}$). Thus, Rsph1$^{/}$ mice display a PCD phenotype similar to but less severe than that observed in Dnaic1$^{/}$ mice, similar to what has been observed in humans. The results suggest that some individuals with PCD may not have a complete loss of mucociliary clearance and further suggest that early diagnosis and intervention may be important to maintain this low amount of clearance.

FULL TEXT

Primary ciliary dyskinesia (PCD) is a rare genetic disease that occurs with an estimated incidence of approximately 1:10,000–1:16,000 (1). The disease is usually inherited in an autosomal recessive pattern and is caused by mutations that disrupt the function of motile cilia, in particular those of the respiratory tract. Motile cilia possess the same basic axonemal structure that is conserved among cilia and flagella from a wide variety of organisms and consists of a central pair of microtubules surrounded by nine uniformly spaced microtubule doublets. Each outer doublet is connected to the adjacent doublet by a series of inner dynein arms and outer dynein arms (ODAs) that provide the force for ciliary motion, and each outer doublet is connected to the central pair by radial spokes. Although the basic “9 + 2” structure appears relatively simple, each different type of cilium is specialized for its particular function, and each is composed of more than 250 different proteins (2–5). It is not surprising, therefore, that PCD is genetically heterogeneous, because mutations in many of these proteins have been shown to disrupt ciliary function. PCD-causing mutations have been identified in over 40 different genes to date, and these do not account for all cases of PCD, indicating that additional PCD-causing mutations are yet to be found. Many of the genes identified are structural components of the ciliary axoneme. For example, *DNAI1* (dynein axonemal intermediate chain 1) and *DNAH5* are components of the ODA, and mutations in these genes typically result in the loss of the ODA and reduced or absent ciliary beat frequency (CBF) (6–10). However, mutations in nonaxonemal proteins, including those involved in dynein arm assembly (e.g., DNAAF1 [dynein, axonemal, assembly factor 1],

HEATR2 [heat repeat-containing protein 2], SPAG1 [sperm-associated antigen 1]) have also been identified as causes of PCD (11–13).

The disruption of motile cilia function results in a broad spectrum of disease symptoms in individuals with PCD (14–17). The lack of effective mucociliary clearance (MCC) in the respiratory tract is responsible for much of the associated morbidity, including recurrent lower respiratory infections, chronic cough, chronic rhinosinusitis, and otitis media. A delayed onset of neonatal respiratory distress has been reported to occur in many infants with PCD, although the mechanism is currently unknown (18). Bronchiectasis occurs at an early age in patients with PCD, and, in severe cases, the frequent and recurring pulmonary infections can result in respiratory failure, with a lung transplant as the only remaining treatment option. Male individuals with PCD are typically infertile, and there is some evidence that females may exhibit reduced fertility. In addition, a subset of patients with mutations that affect the nodal cilia exhibit a spectrum of laterality defects (19, 20).

Although most individuals with PCD exhibit a similar clinical phenotype that can be explained by defective ciliary motility, individuals vary in both the spectrum and severity of disease. For example, we have previously reported that individuals with mutations in *RSPH1* (radial spoke head homolog 1) have a milder course of disease than individuals with PCD with mutations in other genes (21). Individuals with *RSPH1* mutations had fewer incidences of neonatal respiratory distress, higher concentrations of nasal nitric oxide, and better lung function, as measured by forced expiratory volume in 1 second. A significant percentage of ciliary axonemes from individuals with PCD with *RSPH1* mutations appear normal by transmission EM and maintain an almost normal CBF, but these axonemes have been observed to beat in a circular pattern (21–23). Together, these results suggest that the ciliary activity observed in individuals with *RSPH1* mutations may provide a reduced, but significant, amount of MCC. This contrasts with PCD cases in which the cilia are immotile or dyskinetic and are incapable of providing any effective MCC. Alternatively, the difference in clinical phenotype may be a result of other causes, including genetic modifiers or environmental factors.

To further test the hypothesis that *RSPH1* mutations result in some amount of MCC and a less severe PCD phenotype, as well as to gain insights into the mechanisms that may be responsible, we have characterized the pathogenesis of disease in a mouse model with a deletion of *Rsph1* (24). We also compared the *Rsph1*$^{-/-}$ mice with animals with a deletion of dynein axonemal intermediate chain 1 (*Dnaic1*$^{-/-}$) that causes ciliary immotility and a complete lack of effective MCC (25). Our results show that *Rsph1*$^{-/-}$ mice demonstrate significant ciliary activity and a low amount of mucociliary transport at young ages (Days 3–11), but mucociliary transport ceases by Day 30. In addition, the *Rsph1*$^{-/-}$ mice also showed a reduced amount of nasal bacterial colonization at early time points compared with the *Dnaic1*$^{-/-}$ mice. These data support the hypothesis that although mutations in *RSPH1* disrupt ciliary function and cause PCD in humans, the residual ciliary activity results in a less severe clinical phenotype.

Methods

Generation, Breeding, Maintenance of Mice

Rsph1$^{-/-}$ mice were obtained from the Riken BioResource Center. These animals carry a neomycin insertion that replaces exons 1–3 of the *Rsph1* gene (24) and were maintained on a mixed C57BL6/129 background. *Dnaic1*$^{-/-}$ animals were also maintained on a mixed C57BL6/129 background as previously described (25). Heterozygous animals were mated to produce wild-type (WT), heterozygous, and homozygous null (*Rsph1*$^{-/-}$) animals for study. No differences between WT and heterozygous animals were observed, and both were used as controls. Animals were genotyped using standard PCR protocols with primers listed in Table E1 in the data supplement. All studies were conducted under protocols approved by the University of North Carolina Institutional Animal Care and Use Committee.

Cell Culture and Analysis of Expression

Mouse tracheal epithelial cells (MTECs) were isolated and cultured at the air–liquid interface on collagen-coated Millicells (12 mm, 0.4 m; MilliporeSigma) as described previously (26). Total RNA was isolated from differentiated cultures of MTECs isolated from WT or *Rsph1*$^{-/-}$ animals. RT-PCR was performed using *Rsph1*-specific primers, and primers specific for *Dnaic1* were used as a positive control for RNA quality (Table E1).

Ciliary Structure Analysis

Tracheas from adult (6.5 mo old) WT ($n = 2$), heterozygous ($n = 2$), and *Rsph1*$^{-/-}$ ($n = 3$) animals were fixed in an excess of 2% paraformaldehyde, 2% glutaraldehyde with 1% tannic acid for at least 24 hours. Tissue was processed according to published protocols, and high-quality images of axonemal cross-sections were obtained (27). Images from 398 control and 228 *Rsph1*$^{-/-}$ ciliary cross-sections were evaluated for structural aberrations. Relative alignment of cilia was determined in the same micrographs by drawing a line connecting the two central pair microtubules and calculating the mean vector. Additional details are provided in the data supplement.

Measurement of CBF

MTECs were isolated and cultured as above, and ciliary activity was visualized with a Nikon Eclipse TE2000 inverted microscope (Nikon Instruments Inc.) using phase optics and a 20× objective. A Redlake ES-310T camera driven by SAVA software (28) (Ammons Engineering) was used to record and measure CBF as previously described (29). Briefly, 10–12 alternating microscopic fields were recorded from each culture and analyzed using the whole-field analysis option in SAVA. Cultures analyzed for CBF exhibited high amounts of ciliary activity (>40% active area as measured by SAVA).

Analysis of Ciliary Waveform

To examine ciliary waveform, the nasal septum was dissected from adult littermate control and *Rsph1*$^{-/-}$ animals. The ciliated epithelium was peeled from the nasal cartilage and placed in a culture dish containing F12 media. A chamber was constructed around the sample using three No. 1 coverglasses (18 × 18 mm) held together with silicone grease. The chamber channel had a cross-section of 16 mm × 200 m and had open ends to flush the sample with fresh F12. The chamber was placed on a Nikon Eclipse inverted microscope and imaged with a 60× oil objective (plan achromat; numerical aperture, 1.4), a high–numerical aperture (0.85) air condenser, and differential interference contrast optics. A postobjective optical magnification of 1.5× was also applied. The transmitted light was recorded using a Basler acA1300-200um camera under the control of SAVA software. Videos of 1,024 frames were taken at 300 frames/s. Post-processing of the images was used to increase the contrast. Videos were then replayed in slow motion and analyzed by an investigator blinded to the genotype of the animals (30). Cilia were tracked by manually marking *x, y* coordinates of cilia while visually inspecting video frames. Three cilia from one video were tracked for each mouse, and the direction of the ciliary beat was noted. From these data, the end-recovery position and central beat axis were calculated. The maximal distance (d) from a ciliary position to the central axis was calculated and used to compare genotypes.

Measurement of MCC

MCC in the nasal cavity was measured as previously described (31). Briefly, animals were anesthetized with 2.5% isoflurane and then killed by aortic exsanguination. The lower jaw was removed; a small incision was made in the lateral wall of the anterior nasopharynx; and a silica cannula was used to introduce a small amount of dry fluorescent 7-m beads (Thermo Fisher Scientific). The preparation was placed under a dissecting microscope with a fluorescent lamp outfitted with a video camera (MTI), and the rate of MCC was determined by measuring the time it took fluorescent particles to traverse a calibrated distance in the anterior nasopharynx. Usually, 10–30 particles were tracked per mouse over a 10-minute period. The analysis was performed by an investigator blinded to the animals' genotype.

Nasal Bacterial Counts

The nasal septum was dissected starting approximately 3 mm from the tip of the mouse nose up to the ethmoid bone under sterile conditions, transferred to a centrifuge tube containing 0.2 ml of sterile PBS, and vigorously vortexed for 30 seconds. Serial dilutions (1:1, 1:10, 1:100) were plated on Columbia anaerobic sheep blood agar plates (BD Biosciences) and incubated in microaerophilic conditions at 37°C, as described previously (32). Colony-forming units were counted after 18–24 hours of incubation.

Quantification of Bronchus-Associated Lymphoid Tissue

Lungs from control and *Rsph1*$^{-/-}$ animals were fixed with 10% neutral-buffered formalin, and paraffin sections were prepared. Each lobe was sectioned longitudinally to maximize airways, and hematoxylin and eosin–stained

sections were examined by light microscopy to identify foci of bronchus-associated lymphoid tissue (31).

Results

To investigate the consequences of *Rsph1* deletion on ciliary structure and function in a mammalian model, we obtained transgenic mice carrying a deletion of exons 1–3 in the *Rsph1* gene (1). The mice were maintained on a mixed C57BL6/129 background, and heterozygote animals were bred to generate WT, heterozygote, and homozygous *Rsph1*$^{-/-}$ animals. Although not noted in the original report, we observed that *Rsph1*$^{-/-}$ animals developed various degrees of hydrocephalus, similar to other mouse models of PCD, although many animals survived into adulthood (33). Of 155 *Rsph1*$^{-/-}$ animals that were not used for experimental studies or killed for humane reasons, 48 animals survived longer than 30 days. This is a much higher percentage (30%) than what we have observed in the *Dnaic1*$^{-/-}$ mouse line (25). Animals that are *Dnaic1*$^{-/-}$ at birth seldom survive past 1 week (W. Yin and L. Ostrowski, unpublished results). To confirm that the deletion resulted in the complete loss of *Rsph1* expression in the airways, we performed RT-PCR on differentiated cultures of MTECs using primers specific for *Rsph1*. Although cells from control animals exhibited a strong positive signal, cells from the *Rsph1*$^{-/-}$ mice produced no detectable signal, confirming that the deletion eliminated the expression of *Rsph1* (Figure E1). We also performed Western blotting of tracheal extracts with a rabbit polyclonal anti-RSPH1 antibody (Figure E2). As expected, no protein was detected in the *Rsph1*$^{-/-}$ samples, whereas samples from WT animals produced a clear signal.

To examine the effect of *Rsph1* deletion on the structure of the motile cilia in the airways, tracheas from control and mutant animals were examined by transmission EM. Ninety-eight percent (390 of 398) of ciliary cross-sections examined from control animals showed a normal, 9 + 2 axonemal structure (Figures 1A and 1B). In contrast, only 50% (113 of 228) of the cilia from the *Rsph1*$^{-/-}$ animals were scored as normal. The most common abnormality observed, occurring in 52% of the abnormal axonemes (60 of 115), was a transposition defect, in which the central pair is missing and one of the outer doublets has migrated into the central region of the axoneme (Figures 1A and 1B). Other ciliary abnormalities observed included a missing central pair (28 of 115 [24%]) and translocations (7 of 115 [6%]) (Figures 1A and 1B). These results are similar to observations in human patients with PCD with mutations in *RSPH1* (34).

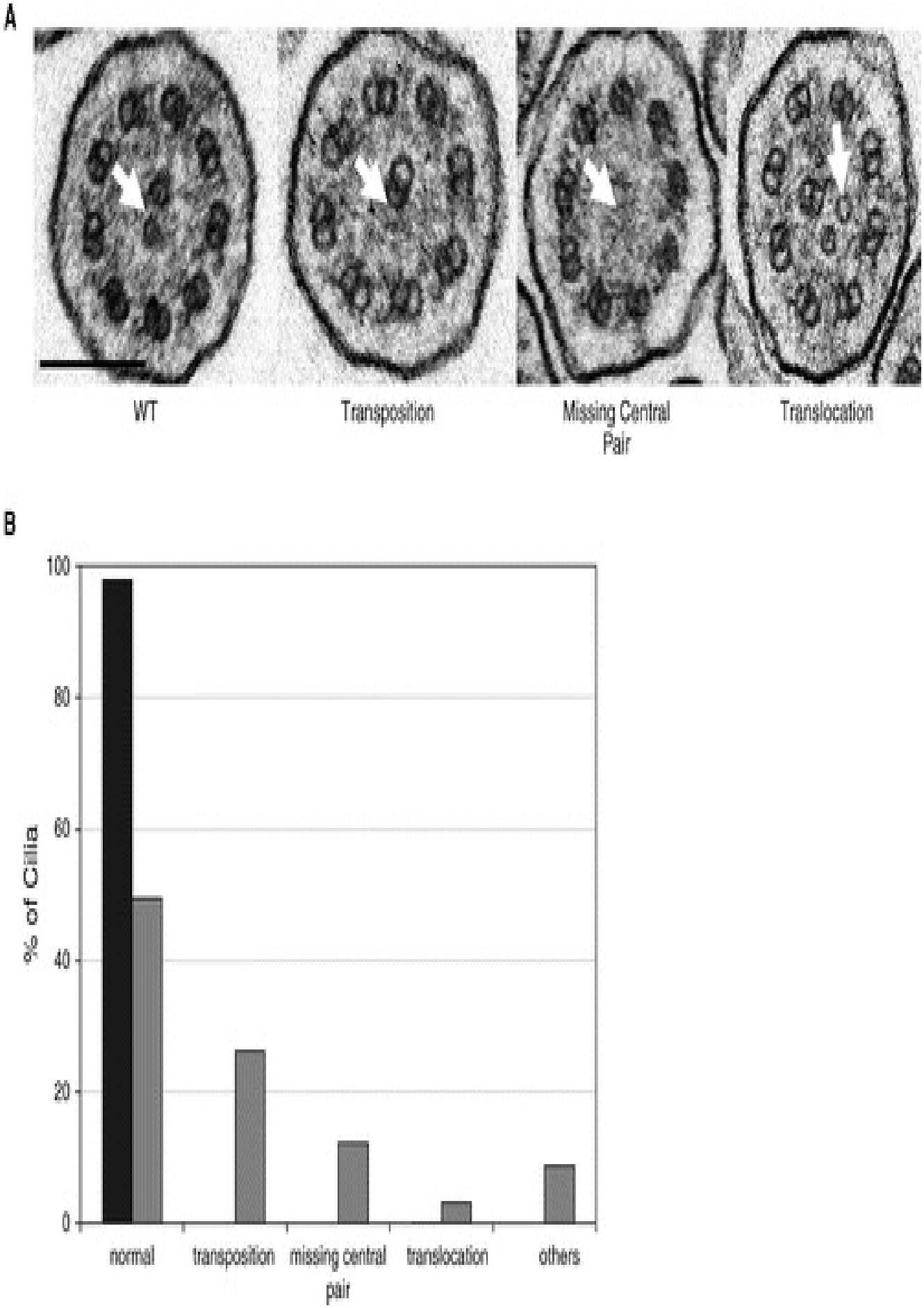

Enlarge this image.

To examine the orientation of the *Rsph1*$^{-/-}$ cilia, we measured the alignment of the central pair between cilia in the same micrographs and calculated the mean vector length. Cilia from the control animals appeared well aligned,

with an overall mean vector length of 0.86 (weighted average of 502 cilia) (Figure 2A). Cilia from the *Rsph1*$^{/}$ animals appeared less well aligned (Figure 2B), although some images showed high local alignment (Figure 2C). The mean vector length of the *Rsph1*$^{/}$ cilia was 0.74, measured from the cilia with a normal central pair (weighted average of 179 cilia). We also observed a similar pattern of ultrastructural defects in cilia from MTECs cultured at the air–liquid interface. Cilia from WT cultures showed a normal 9 + 2 axoneme (113 of 113 [100%]), whereas approximately 30% (42 of 135) of cilia from *Rsph1*$^{/}$ cultures were abnormal. The abnormal cilia showed the same defects as cilia from the intact trachea, with 17 of 42 abnormal axonemes (40%) showing a transposition defect and 23 of 42 abnormal axonemes (55%) missing the central pair. These data confirm that the defects observed are genetic in nature and are not secondary to the PCD phenotype.

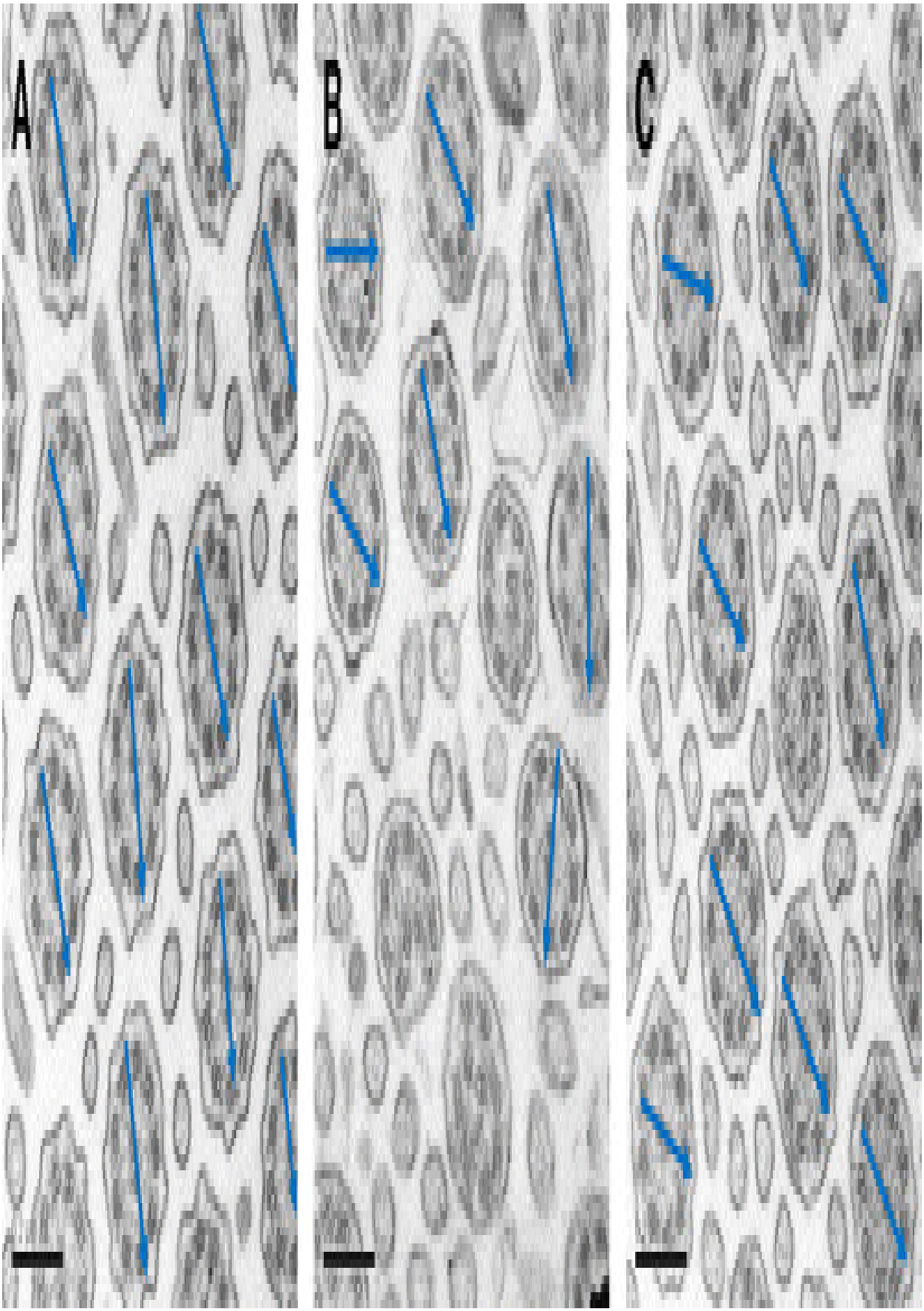

Enlarge this image.

Airway epithelial cells from individuals with PCD caused by mutations in *RSPH1* have been reported to exhibit normal or reduced CBF (21, 23, 35). To determine the effect of *Rsph1* deletion on ciliary activity in the mouse

model, MTECs were cultured at the air–liquid interface until ciliated cell differentiation occurred. Measurement of CBF by high-speed video microscopy and whole-field analysis using the SAVA software system (28) showed that *Rsph1* deletion resulted in a significantly reduced CBF. At 37°C, CBF was reduced from 25.0 ± 0.9 Hz in the control cultures to 20.2 ± 0.8 Hz in the *Rsph1*$^{-/-}$ cultures ($P < 0.003$; average ± SD; $n = 3$). Although the reduction in CBF was significant, cilia from the *Rsph1*$^{-/-}$ mice exhibited abundant ciliary activity, especially when compared with cilia from mouse models with mutations in other PCD-causing genes that result in essentially immotile cilia (e.g., *Dnah5*, *Dnaic1* [25, 36]).

To determine the effect of *Rsph1* deletion on ciliary waveform, we isolated sheets of ciliated epithelium from the nasal septum and recorded high-speed videos at high magnification using differential interference contrast (37). When analyzed in a slow-motion replay, cilia from the *Rsph1*$^{-/-}$ animals were observed to exhibit a slightly circular (counterclockwise) waveform that was distinct from that of the control samples (Figure 3 and Videos E1 and E2). Measuring the distance that the ciliary beat deviated from planar revealed a clear difference between the control and *Rsph1*$^{-/-}$ animals (control vs. *Rsph1*$^{-/-}$, 0.43 m vs. 1.05 m; $P < 0.004$; $n = 36$). This circular waveform has previously been observed in samples from human subjects with mutations in radial spoke proteins (e.g., 21, 23, 34, 38). Thus, the deletion of *Rsph1* has an effect on ciliary activity in the mouse similar to that in humans.

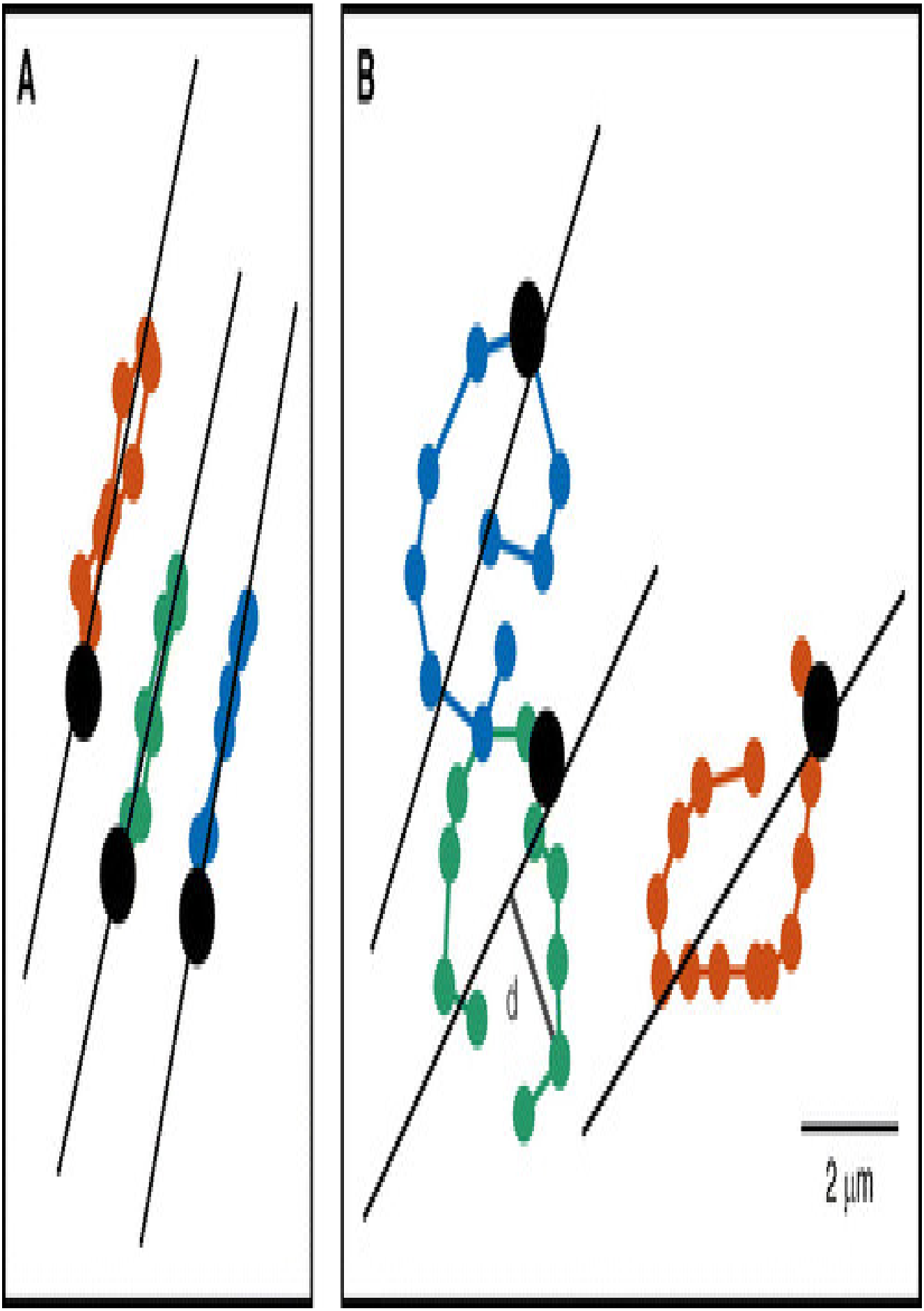

Enlarge this image.

As noted above, individuals with PCD caused by mutations in *RSPH1* have been observed to have a less severe course of disease than that observed in individuals with other mutations. To test the hypothesis that mutations in

RSPH1 may reduce but not eliminate MCC, we measured the rate of MCC in the nasopharynx of control and *Rsph1*$^{-/-}$ animals. The rate of MCC was measured in mice of different ages by recording the movement of fluorescent beads in the anterior nasopharynx, as described previously (31). In control animals, the rate of MCC increased between Days 1 and 30 (Figure 4). Similar observations have been reported in the trachea, where both the extent of ciliation and the speed of cilia-generated flow were reported to increase from Days 1 to 9 after birth (39). Although the rate of MCC also increased in the *Rsph1*$^{-/-}$ group during the first 2 weeks after birth, at each age examined, the rate of MCC in the *Rsph1*$^{-/-}$ mice was significantly less than that in the control mice, being barely detectable at Day 1 and only approximately 20% of control at age 3–4 days and age 10–11 days. Furthermore, in older animals (30 d old), *Rsph1*$^{-/-}$ animals had no measurable MCC, whereas control animals of the same age had a rate of MCC of 8.7 ± 1.1 mm/min (average ± SEM) (Figure 4). As an additional control, we measured MCC in *Dnaic1*$^{-/-}$ animals at similar ages (3–4 d, $n = 3$; 7–11 d, $n = 6$; and 30 d, $n = 1$). As expected, none of these animals exhibited any MCC. These data demonstrate that the deletion of *Rsph1* reduces but does not completely prevent MCC in early postnatal life. The results further suggest that as disease pathogenesis progresses, the accumulated mucus (*see below*) and its sequelae eventually result in the complete cessation of transport.

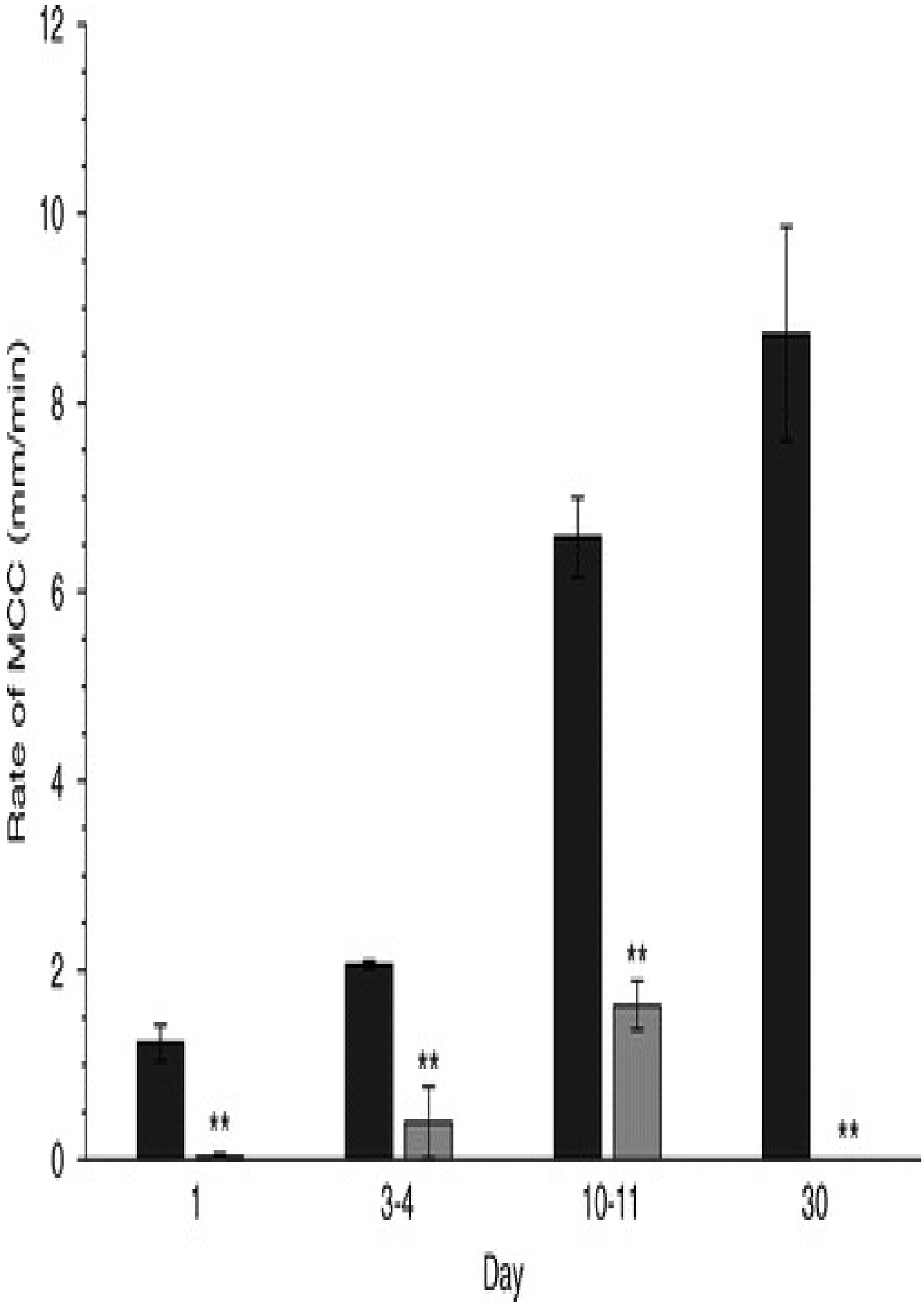

Enlarge this image.

Histological examination of *Rsph1*$^{/}$ animals revealed an accumulation of mucus throughout the nasal cavity, including the regions of the dorsal meatus and ethmoturbinates, as well as the maxillary sinus (Figure 5). The

mucus accumulation appeared to be milder in the younger animals (Figures 5B and 5D), with only small areas affected. In the older animals, the areas of mucus accumulation were larger, and more areas of the nasal cavity were involved (Figures 5F and 5H). Tissue remodeling was also apparent in the older animals, with degeneration of the ethmoturbinates frequently observed (Figure 5H). Therefore, even though young *Rsph1*$^{-/-}$ mice have a measurable rate of MCC, it is not sufficient to prevent the accumulation of mucus and initiation of pathogenesis. Histological examination of lung sections collected from age-matched control and *Rsph1*$^{-/-}$ animals revealed no obvious mucus accumulation or other pathology in the PCD animals. Although a preliminary report suggested a higher incidence of bronchus-associated lymphoid tissue in the *Rsph1*$^{-/-}$ mice (40), examination of a larger group of animals (32 control, 29 *Rsph1*$^{-/-}$) did not show a significant difference (Figure E3).

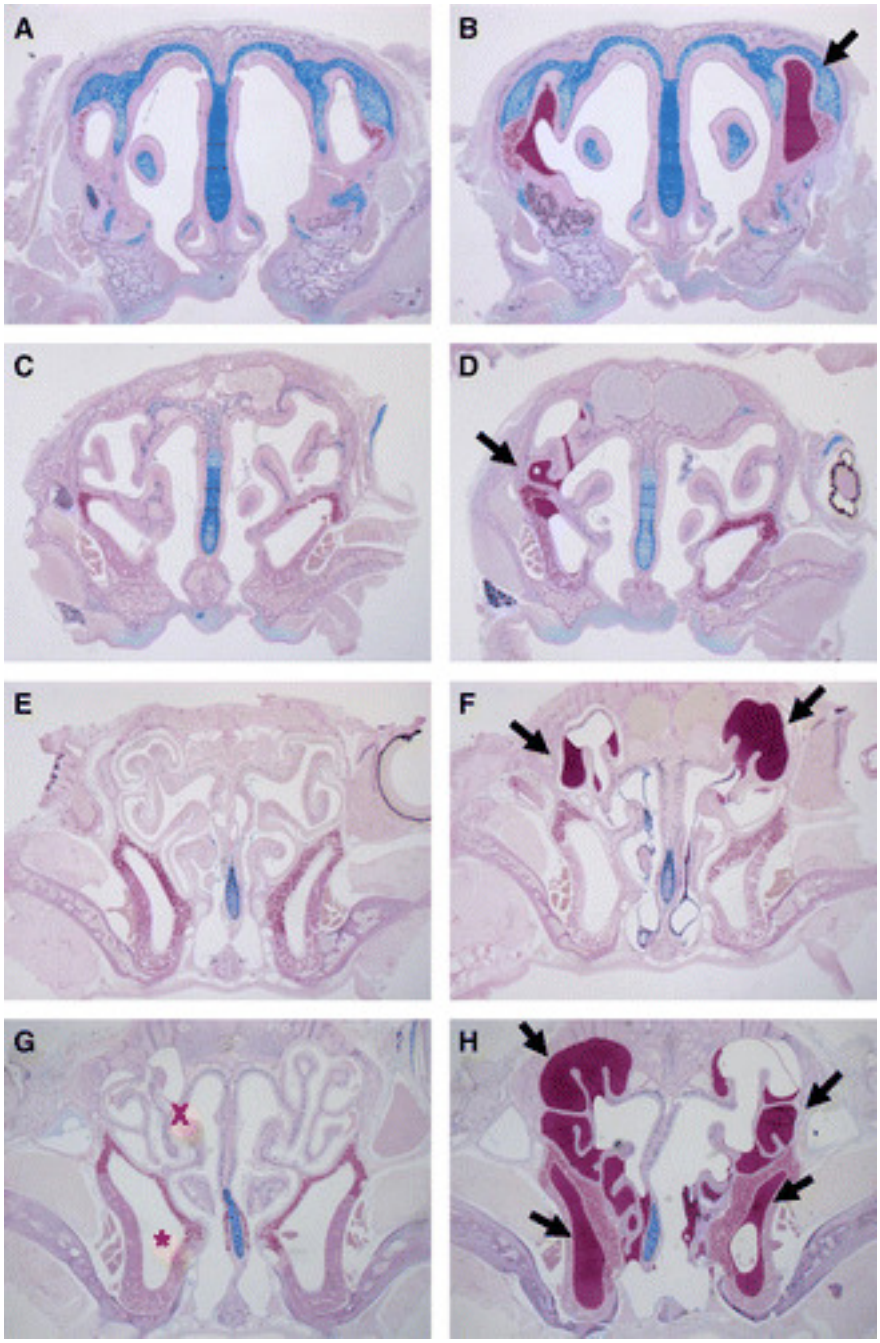

Enlarge this image.

To further examine the pathogenesis of PCD in the *Rsph1*$^{-/-}$ mice, we quantified the bacterial load in the nasal cavity of control and PCD mice in two different age groups: Days 4–10 (when the *Rsph1*$^{-/-}$ animals showed some MCC) and at an older age, Days 21–46 (Figure 6). To compare the phenotype of the *Rsph1*$^{-/-}$ mice with that of animals with immotile cilia, we also quantified the bacterial load in *Dnaic1*$^{-/-}$ animals. The number of *Dnaic1*$^{-/-}$ animals studied

was limited because the majority of these animals die shortly after birth. Although the *Rsph1*$^{-/-}$ animals showed a trend toward an increased number of bacteria, the average number of bacterial colonies was not significantly different from that seen in the control WT animals in either group (*Rsph1*$^{-/-}$ vs. control, 641 ± 267 vs. 181 ± 107 at Days 4–10; and *Rsph1*$^{-/-}$ vs. control, 296 ± 181 vs. 47 ± 42 at Days 21–46 [average ± SEM]). In contrast, all *Dnaic1*$^{-/-}$ animals had many culturable bacteria at both time points ($5.6 \times 10^5 \pm 1.3 \times 10^5$ at Days 4–10 and $1.2 \times 10^4 \pm 2.8 \times 10^3$ at Days 21–46 [average ± SEM]), and the difference in colony-forming units was highly significant versus the control and *Rsph1*$^{-/-}$ animals at both times ($P < 0.002$ for each).

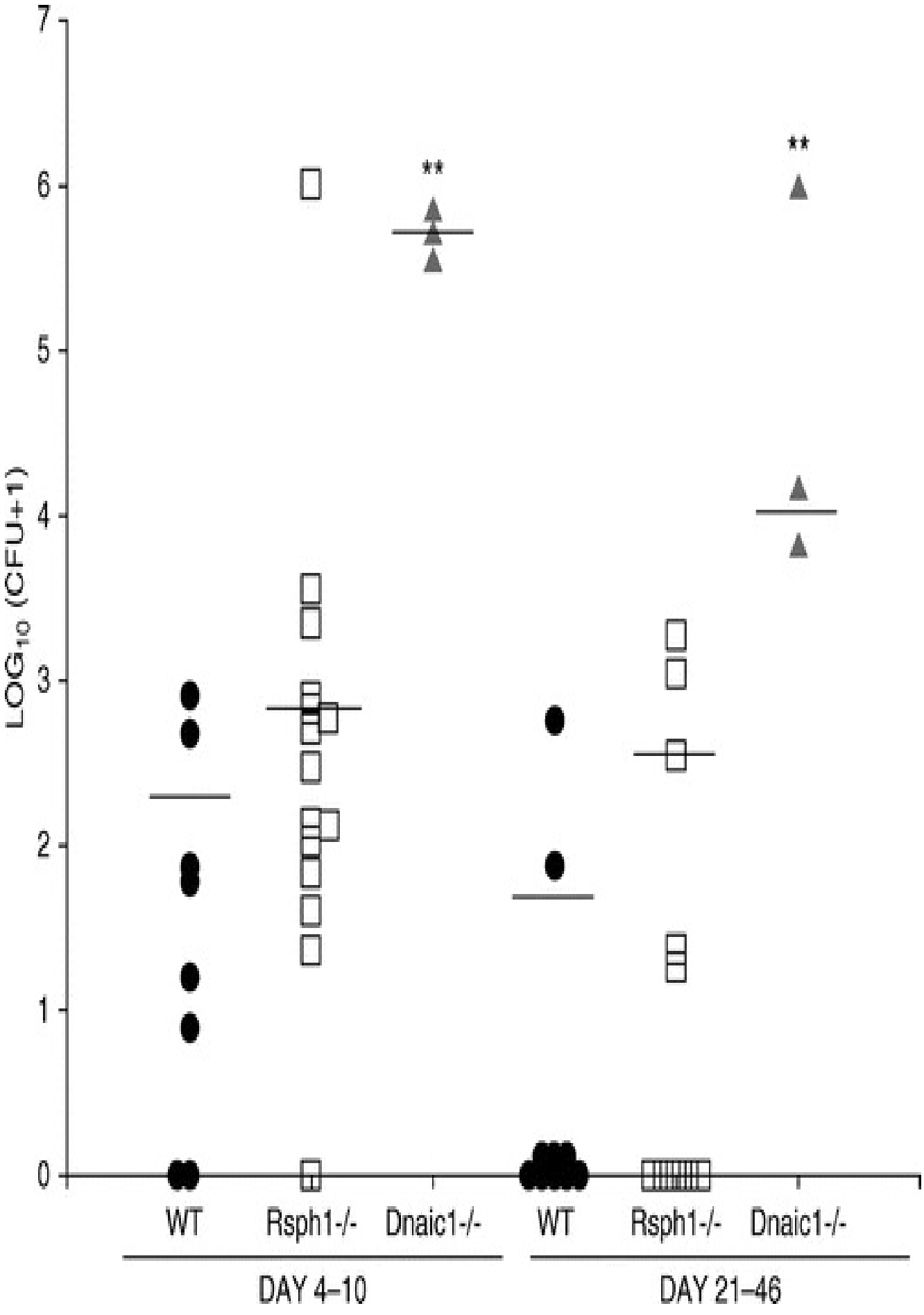

Enlarge this image.

Discussion

PCD is a genetically heterogeneous disease, with causative mutations identified in more than 40 genes to date.

This is not surprising when one considers that motile cilia of the respiratory tract consist of more than 250 unique proteins, many of them expressed only in ciliated cells. In general, a mutation that causes a defect in ciliary function would be expected to cause the same or a very similar phenotype, and this is in fact what is observed, with most individuals with PCD exhibiting common symptoms, including chronic rhinosinusitis, otitis media, chronic cough, pneumonia, and bronchiectasis. However, PCD is also phenotypically heterogeneous, with some individuals having severe life-shortening airway disease and others experiencing less severe symptoms. Because PCD is a rare disease, the number of individuals with mutations in the same gene is small, and the number of individuals with the same pair of causative mutations is even smaller. Thus, investigations into the relationships between genotype and phenotype have been limited. However, with the increasing availability of genetic testing to diagnose PCD, some genotype–phenotype associations have become apparent. For example, individuals with PCD caused by mutations in *CCDC39* or *CCDC40* (coiled-coil domain-containing 39 or 40, respectively) have worse lung disease than those with ODA or ODA and inner dynein arm defects (14). We previously reported that individuals with mutations in *RSPH1* had a less severe phenotype than a group of individuals with "classic" PCD caused by mutations in genes other than *RSPH1* (21). Individuals with *RSPH1* mutations had fewer incidences of neonatal respiratory distress, higher concentrations of nasal nitric oxide, and statistically higher lung function, as measured by forced expiratory volume in 1 second. We demonstrated that *RSPH1*-mutant cilia had significant ciliary activity, appearing to beat in a circular pattern, similar to nodal cilia. An average of 80% of ciliary cross-sections obtained by transmission EM from individuals with mutations in *RSPH1* had a normal 9 + 2 axonemal structure, whereas only 50% of individuals with mutations in *RSPH4A* (radial spoke head 4, *Chlamydomonas*, homolog of, A) appeared as normal (34). These results suggested that the residual ciliary activity was sufficient to modify the severity of disease pathogenesis in patients with *RSPH1* mutations. To increase understanding of ciliary structure–function and genotype–phenotype relationships in PCD, we characterized a mouse model with a deletion of the mouse homolog of *RSPH1*.

Analysis of tracheal cilia from *Rsph1*$^{-/-}$ mice by transmission EM revealed a spectrum of abnormalities. Approximately 50% of the ciliary cross-sections examined appeared normal, whereas approximately 25% showed an 8 + 1 structure, with a transposition of one of the outer doublets into the central regions. Other ciliary defects observed included axonemes with a missing central pair (10%) or the translocation of an outer doublet into the midregion of the axoneme (3%). This spectrum of abnormalities is similar to that observed in human patients with PCD with *RSPH1* mutations. For example, in our cohort of 15 subjects with PCD with *RSPH1* mutations, 62–93% of ciliary cross-sections had a normal 9 + 2 structure (21). Kott and colleagues identified 11 subjects with PCD with *RSPH1* mutations and observed a range of 30–81% normal axonemal structure (35). Onoufriadis and colleagues reported similar results for a small number of patients (23). It is now clear from a number of studies that disruption of the radial spoke complex results in an apparent destabilization of the 9 + 2 axonemal structure, resulting in the loss of the central pair and the transposition or translocation of the outer doublets (34, 35, 38, 41). It is also clear that cross-sections of cilia with radial spoke defects obtained by standard transmission EM can appear normal or disrupted, depending on the level of the section in the cilium (23, 42, 43).

Radial spokes are multiprotein complexes consisting of at least 23 proteins and at least three nonidentical structures. The structure of the radial spoke complex cannot be visualized clearly by standard transmission EM, and therefore the specific structural defect caused by the absence of Rsph1 is also not clear. In an immunofluorescence study, Frommer and colleagues (22) reported that subjects with mutations in *RSPH1* also failed to incorporate RSPH9 into their cilia, whereas Jeanson and colleagues reported that a subject with mutations in *RSPH3* (a stalk protein) exhibited positive staining for RSPH1 (41). Our cryo-EM tomography study revealed that cilia isolated from nasal cultures of an *RSPH1*-mutant individual were missing two of the three radial spoke heads present in human ciliary axonemes (44). Additional studies are needed to fully delineate the structure of the radial spokes and the effect of different PCD-causing mutations.

Examination of cultured tracheal epithelial cells from the *Rsph1*$^{-/-}$ animals showed robust ciliary activity, although CBF was consistently lower than in the control animals. This is also consistent with results from human studies, in

which patients with *RSPH1* mutations had, on average, a reduced CBF compared with control subjects (21, 23, 35). In cultured nasal epithelial cells from a subject with PCD with *RSPH1* mutations, we reported that the ciliated cells exhibited a circular clockwise beat pattern (21). Several other studies have also reported that cilia with defects in radial spokes exhibit a circular rotation pattern (23, 34, 38, 42, 45). Examination of ciliary waveform in the nasal epithelia revealed that cilia from the *Rsph1*$^{-/-}$ animals also beat with an aberrant circular pattern. This circular rotation pattern of ciliary axonemes in the absence of radial spokes resembles what is observed in nodal cilia. Shinohara and colleagues (46) reported that cilia from *Rsph4a*$^{-/-}$ mice also beat in a circular clockwise pattern. Furthermore, they showed that in the absence of radial spokes, the axoneme is less stable and more likely to become structurally disorganized when challenged with taxol. Although the mechanism is unclear, these data are consistent with the concept that the presence of radial spokes is required to maintain proper 9 + 2 organization of the ciliary axoneme and the planar beating of airway cilia.

Similar to other murine models of PCD (33, 36), some of the *Rsph1*$^{-/-}$ mice developed hydrocephalus at an early age, and they were killed for humane reasons. However, some of the *Rsph1*$^{-/-}$ animals survived long term (48 of 155 [31%]) and were available for additional studies. Histological analysis revealed mucus accumulation in the nasal cavity of all *Rsph1*$^{-/-}$ animals examined, and the amount of mucus appeared to increase with age. No overt signs of lung disease were observed in the PCD animals, which is consistent with our observations in the *Dnaic1*$^{-/-}$ model (25), and no bacteria were recovered from BAL. This is clearly different from the human condition and likely reflects anatomical differences between mice and humans. None of the animals exhibited situs inversus, which is consistent with the observation that defects in radial spokes do not cause situs abnormalities, because the nodal cilia do not incorporate radial spokes into their 9 + 0 structure.

Interestingly, although older *Rsph1*$^{-/-}$ mice showed no evidence of MCC, analysis of younger animals showed a slow but significant rate of MCC in the nasopharynx. We measured MCC by tracking the distance traveled by fluorescent beads deposited at the anterior tip of the nasopharynx. We have previously reported that in this anatomical location in mice, MCC is particularly robust, even in very young animals (31). Our results demonstrate that in the control animals, the rate of MCC increases with age, possibly due to a progressive increase in the number of ciliated cells, as has been observed in the trachea (39). In the *Rsph1*$^{-/-}$ animals, the rate of MCC also appeared to increase over the first 10 days but was markedly reduced compared with the control animals. Between 10 and 11 days of age, the rate of MCC in the PCD animals was approximately 20% of that in the control animals. Thus, although the absence of Rsph1 clearly results in defective ciliary structure, a reduced CBF, and an aberrant circular waveform, young *Rsph1*$^{-/-}$ mice maintain a low but significant amount of MCC, at least in the nasopharynx. This residual amount of MCC was lost over time, suggesting that it was not sufficient to prevent mucus accumulation and further disease progression in the nasal cavity. Because MCC in the *Rsph1*$^{-/-}$ mice is inefficient, it is possible that mucus simply accumulates until the defective *Rsph1*$^{-/-}$ cilia can no longer provide enough force to maintain MCC. It is also possible that the properties of the mucus itself may be different in older animals, owing to developmental changes or in response to environmental challenges. For example, we have observed that the abundance of mucous secretory cells in the trachea and bronchi of neonatal mice is altered in a reproducible developmental pattern between Days 5 and 10 (47). Alternatively, the presence of accumulated mucus may itself trigger a response that alters the composition and properties of airway secretions in the older *Rsph1*$^{-/-}$ animals. Although it is not clear why MCC ceases in the *Rsph1*$^{-/-}$ mouse model, the initial low amount of MCC may explain the less severe phenotype of PCD in patients with *RSPH1* mutations. Although mutations in *RSPH1* disrupt the axonemal structure of respiratory cilia and alter the beat pattern from planar to circular, it is possible that, similarly to the 9 + 0 cilia of the node, the *RSPH1*-mutant cilia may still be able to generate directional flow. This is in fact what we have observed in the mouse model, where a low amount of MCC was present in the nasopharynx of young mice. However, other mechanisms may also be involved. The near-normal CBF of *RSPH1*-mutant cilia may stimulate the production of NO, which may then act as an antimicrobial or bronchodilator (48, 49). Alternatively, the *RSPH1*-mutant cilia may retain other sensing or signaling functions that might mitigate disease symptoms. For example, Button and colleagues reported that ciliated cells sense the hydration state of the overlying mucus layer

(50), and Shah and colleagues reported that human ciliated cells express sensory bitter taste receptors (51). It would be interesting to perform studies of MCC in subjects with *RSPH1* and other radial spoke mutations, especially in younger individuals, to determine directly if they exhibit a significant amount of MCC. It will also be of interest to determine if treatment of young *Rsph1*$^{-/-}$ mice with therapies to clear mucus (e.g., mucolytics or nasal lavage with normal or hypertonic saline) might improve the rate and/or prolong the duration of MCC. Finally, although there are many benefits to early diagnosis and treatment of PCD, the development of treatments to improve or maintain low amounts of MCC, if present, in patients with *RSPH1* mutations may provide an even greater therapeutic benefit.

References

1. Zariwala MA, Knowles MR, Leigh MW. Primary ciliary dyskinesia. In: Adam MP, Ardinger HH, Pagon RA*et al.*, editors. GeneReviews [Internet]. Seattle, WA: University of Washington; 2007 Jan 24 [updated 2015 Sep 3].
2. Blackburn K, Bustamante-Marin X, Yin W, Goshe MB, Ostrowski LE. Quantitative proteomic analysis of human airway cilia identifies previously uncharacterized proteins of high abundance. *J Proteome Res* 2017;16:1579–1592.
3. Dutcher SK. Flagellar assembly in two hundred and fifty easy-to-follow steps. *Trends Genet* 1995;11:398–404.
4. Ostrowski LE, Blackburn K, Radde KM, Moyer MB, Schlatzer DM, Moseley A*et al.* A proteomic analysis of human cilia: identification of novel components. *Mol Cell Proteomics* 2002;1:451–465.
5. Pazour GJ, Agrin N, Leszyk J, Witman GB. Proteomic analysis of a eukaryotic cilium. *J Cell Biol* 2005;170:103–113.
6. Guichard C, Harricane MC, Lafitte JJ, Godard P, Zaegel M, Tack V*et al.* Axonemal dynein intermediate-chain gene (DNAI1) mutations result in situs inversus and primary ciliary dyskinesia (Kartagener syndrome). *Am J Hum Genet* 2001;68:1030–1035.
7. Hornef N, Olbrich H, Horvath J, Zariwala MA, Fliegauf M, Loges NT*et al.* DNAH5 mutations are a common cause of primary ciliary dyskinesia with outer dynein arm defects. *Am J Respir Crit Care Med* 2006;174:120–126.
8. Olbrich H, Häffner K, Kispert A, Völkel A, Volz A, Sasmaz G*et al.* Mutations in DNAH5 cause primary ciliary dyskinesia and randomization of left-right asymmetry. *Nat Genet* 2002;30:143–144.
9. Pennarun G, Escudier E, Chapelin C, Bridoux AM, Cacheux V, Roger G*et al.* Loss-of-function mutations in a human gene related to *Chlamydomonas reinhardtii* dynein IC78 result in primary ciliary dyskinesia. *Am J Hum Genet* 1999;65:1508–1519.
10. Zariwala M, Noone PG, Sannuti A, Minnix S, Zhou Z, Leigh MW*et al.* Germline mutations in an intermediate chain dynein cause primary ciliary dyskinesia. *Am J Respir Cell Mol Biol* 2001;25:577–583.
11. Horani A, Ferkol TW, Brody SL. HEATR2, a novel candidate for primary ciliary dyskinesia is required for ciliary motor protein assembly and function []. *Am J Respir Cell Mol Biol* 2012;185:A2484.
12. Knowles MR, Ostrowski LE, Loges NT, Hurd T, Leigh MW, Huang L*et al.* Mutations in SPAG1 cause primary ciliary dyskinesia associated with defective outer and inner dynein arms. *Am J Hum Genet* 2013;93:711–720.
13. Omran H, Kobayashi D, Olbrich H, Tsukahara T, Loges NT, Hagiwara H*et al.* Ktu/PF13 is required for cytoplasmic pre-assembly of axonemal dyneins. *Nature* 2008;456:611–616.
14. Davis SD, Ferkol TW, Rosenfeld M, Lee HS, Dell SD, Sagel SD*et al.* Clinical features of childhood primary ciliary dyskinesia by genotype and ultrastructural phenotype. *Am J Respir Crit Care Med* 2015;191:316–324.
15. Knowles MR, Daniels LA, Davis SD, Zariwala MA, Leigh MW. Primary ciliary dyskinesia: recent advances in diagnostics, genetics, and characterization of clinical disease. *Am J Respir Crit Care Med* 2013;188:913–922.
16. Knowles MR, Zariwala M, Leigh M. Primary ciliary dyskinesia. *Clin Chest Med* 2016;37:449–461.
17. Leigh MW, Ferkol TW, Davis SD, Lee HS, Rosenfeld M, Dell SD*et al.* Clinical features and associated likelihood of primary ciliary dyskinesia in children and adolescents. *Ann Am Thorac Soc* 2016;13:1305–1313.
18. Mullowney T, Manson D, Kim R, Stephens D, Shah V, Dell S. Primary ciliary dyskinesia and neonatal respiratory distress. *Pediatrics* 2014;134:1160–1166.
19. Kennedy MP, Omran H, Leigh MW, Dell S, Morgan L, Molina PL*et al.* Congenital heart disease and other

heterotaxic defects in a large cohort of patients with primary ciliary dyskinesia. *Circulation* 2007;115:2814–2821.
20. Shapiro AJ, Davis SD, Ferkol T, Dell SD, Rosenfeld M, Olivier KN*et al.*; Genetic Disorders of Mucociliary Clearance Consortium. Laterality defects other than situs inversus totalis in primary ciliary dyskinesia: insights into situs ambiguus and heterotaxy. *Chest* 2014;146:1176–1186.
21. Knowles MR, Ostrowski LE, Leigh MW, Sears PR, Davis SD, Wolf WE*et al.* Mutations in RSPH1 cause primary ciliary dyskinesia with a unique clinical and ciliary phenotype. *Am J Respir Crit Care Med* 2014;189:707–717.
22. Frommer A, Hjeij R, Loges NT, Edelbusch C, Jahnke C, Raidt J*et al.* Immunofluorescence analysis and diagnosis of primary ciliary dyskinesia with radial spoke defects. *Am J Respir Cell Mol Biol* 2015;53:563–573.
23. Onoufriadis A, Shoemark A, Schmidts M, Patel M, Jimenez G, Liu H*et al.*; UK10K. Targeted NGS gene panel identifies mutations in RSPH1 causing primary ciliary dyskinesia and a common mechanism for ciliary central pair agenesis due to radial spoke defects. *Hum Mol Genet* 2014;23:3362–3374.
24. Tokuhiro K, Hirose M, Miyagawa Y, Tsujimura A, Irie S, Isotani A*et al.* Meichroacidin containing the membrane occupation and recognition nexus motif is essential for spermatozoa morphogenesis. *J Biol Chem* 2008;283:19039–19048.
25. Ostrowski LE, Yin W, Rogers TD, Busalacchi KB, Chua M, O'Neal WK*et al.* Conditional deletion of *Dnaic1* in a murine model of primary ciliary dyskinesia causes chronic rhinosinusitis. *Am J Respir Cell Mol Biol* 2010;43:55–63.
26. You Y, Richer EJ, Huang T, Brody SL. Growth and differentiation of mouse tracheal epithelial cells: selection of a proliferative population. *Am J Physiol Lung Cell Mol Physiol* 2002;283:L1315–L1321.
27. Olin JT, Burns K, Carson JL, Metjian H, Atkinson JJ, Davis SD*et al.*; Genetic Disorders of Mucociliary Clearance Consortium. Diagnostic yield of nasal scrape biopsies in primary ciliary dyskinesia: a multicenter experience. *Pediatr Pulmonol* 2011;46:483–488.
28. Sisson JH, Stoner JA, Ammons BA, Wyatt TA. All-digital image capture and whole-field analysis of ciliary beat frequency. *J Microsc* 2003;211:103–111.
29. Ostrowski LE, Yin W, Patel M, Sechelski J, Rogers T, Burns K*et al.* Restoring ciliary function to differentiated primary ciliary dyskinesia cells with a lentiviral vector. *Gene Ther* 2014;21:253–261.
30. Sears PR, Thompson K, Davis CW. Empirical model of the ciliary waveform of human airway epithelium developed using video microscopy. *Mol Biol Cell* 2006;17:2323.
31. Grubb BR, Livraghi-Butrico A, Rogers TD, Yin W, Button B, Ostrowski LE. Reduced mucociliary clearance in old mice is associated with a decrease in Muc5b mucin. *Am J Physiol Lung Cell Mol Physiol* 2016;310:L860–L867.
32. Livraghi-Butrico A, Kelly EJ, Klem ER, Dang H, Wolfgang MC, Boucher RC*et al.* Mucus clearance, MyD88-dependent and MyD88-independent immunity modulate lung susceptibility to spontaneous bacterial infection and inflammation. *Mucosal Immunol* 2012;5:397–408.
33. Lee L. Riding the wave of ependymal cilia: genetic susceptibility to hydrocephalus in primary ciliary dyskinesia. *J Neurosci Res* 2013;91:1117–1132.
34. Daniels ML, Leigh MW, Davis SD, Armstrong MC, Carson JL, Hazucha M*et al.* Founder mutation in *RSPH4A* identified in patients of Hispanic descent with primary ciliary dyskinesia. *Hum Mutat* 2013;34:1352–1356.
35. Kott E, Legendre M, Copin B, Papon JF, Dastot-Le Moal F, Montantin G*et al.* Loss-of-function mutations in RSPH1 cause primary ciliary dyskinesia with central-complex and radial-spoke defects. *Am J Hum Genet* 2013;93:561–570.
36. Ibañez-Tallon I, Gorokhova S, Heintz N. Loss of function of axonemal dynein Mdnah5 causes primary ciliary dyskinesia and hydrocephalus. *Hum Mol Genet* 2002;11:715–721.
37. Sears PR, Thompson K, Knowles MR, Davis CW. Human airway ciliary dynamics. *Am J Physiol Lung Cell Mol Physiol* 2013;304:L170–L183.
38. Castleman VH, Romio L, Chodhari R, Hirst RA, de Castro SC, Parker KA*et al.* Mutations in radial spoke head protein genes RSPH9 and RSPH4A cause primary ciliary dyskinesia with central-microtubular-pair abnormalities. *Am J Hum Genet* 2009;84:197–209.
39. Francis RJ, Chatterjee B, Loges NT, Zentgraf H, Omran H, Lo CW. Initiation and maturation of cilia-generated

flow in newborn and postnatal mouse airway. *Am J Physiol Lung Cell Mol Physiol* 2009;296:L1067–L1075.
40. Ostrowski LE, Livraghi-Butrico A, Yin W, Sears P, Rogers T, Grubb B. Deletion of Rsph1 in a mouse model of primary ciliary dyskinesia results in a mild phenotype []. *Am J Respir Crit Care Med* 2016;193:A5948.
41. Jeanson L, Copin B, Papon JF, Dastot-Le Moal F, Duquesnoy P, Montantin G*et al*. RSPH3 mutations cause primary ciliary dyskinesia with central-complex defects and a near absence of radial spokes. *Am J Hum Genet* 2015;97:153–162.
42. Burgoyne T, Lewis A, Dewar A, Luther P, Hogg C, Shoemark A*et al*. Characterizing the ultrastructure of primary ciliary dyskinesia transposition defect using electron tomography. *Cytoskeleton (Hoboken)* 2014;71:294–301.
43. Zitkiewicz E, Bukowy-Bieryo Z, Voelkel K, Klimek B, Dmeska H, Pogorzelski A*et al*. Mutations in radial spoke head genes and ultrastructural cilia defects in East-European cohort of primary ciliary dyskinesia patients. *PLoS One* 2012;7:e33667.
44. Lin J, Yin W, Smith MC, Song K, Leigh MW, Zariwala MA*et al*. Cryo-electron tomography reveals ciliary defects underlying human RSPH1 primary ciliary dyskinesia. *Nat Commun* 2014;5:5727.
45. Stannard W, Rutman A, Wallis C, O'Callaghan C. Central microtubular agenesis causing primary ciliary dyskinesia. *Am J Respir Crit Care Med* 2004;169:634–637.
46. Shinohara K, Chen D, Nishida T, Misaki K, Yonemura S, Hamada H. Absence of radial spokes in mouse node cilia is required for rotational movement but confers ultrastructural instability as a trade-off. *Dev Cell* 2015;35:236–246.
47. Livraghi A, Grubb BR, Hudson EJ, Wilkinson KJ, Sheehan JK, Mall MA*et al*. Airway and lung pathology due to mucosal surface dehydration in beta-epithelial Na+ channel-overexpressing mice: role of TNF- and IL-4R signaling, influence of neonatal development, and limited efficacy of glucocorticoid treatment. *J Immunol* 2009;182:4357–4367.
48. Ricciardolo FL, Sterk PJ, Gaston B, Folkerts G. Nitric oxide in health and disease of the respiratory system. *Physiol Rev* 2004;84:731–765.
49. Yan CH, Hahn S, McMahon D, Bonislawski D, Kennedy DW, Adappa ND*et al*. Nitric oxide production is stimulated by bitter taste receptors ubiquitously expressed in the sinonasal cavity. *Am J Rhinol Allergy* 2017;31:85–92.
50. Button B, Okada SF, Frederick CB, Thelin WR, Boucher RC. Mechanosensitive ATP release maintains proper mucus hydration of airways. *Sci Signal* 2013;6:ra46.
51. Shah AS, Ben-Shahar Y, Moninger TO, Kline JN, Welsh MJ. Motile cilia of human airway epithelia are chemosensory. *Science* 2009;325:1131–1134.

AuthorAffiliation

Weining Yin, Alessandra Livraghi-Butrico, Patrick R. Sears, Troy D. Rogers, Kimberlie A. Burns, Barbara R. Grubb, and Lawrence E. Ostrowski
Marsico Lung Institute/Cystic Fibrosis Center, University of North Carolina at Chapel Hill, Chapel Hill, North Carolina
Corresponding Author: Lawrence E. Ostrowski